

Cite this: *Mater. Adv.*, 2023,  
4, 5633

## Poly(lactic acid)/wood-based *in situ* polymerized densified composite material†

Akash Madhav Gondaliya,<sup>a</sup> Kieran Foster<sup>b</sup> and E. Johan Foster<sup>id</sup>\*<sup>a</sup>

To develop an advanced wood bio-composite, an economical and energy-efficient manufacturing strategy is showcased in this study. Wood slabs were delignified and impregnated with a simple modifying precursor of lactic acid oligomers. The impregnated wood samples were *in situ* polymerized and densified with heat and pressure, turning the wood into a functionalized densified material. The modified material was confirmed by observing the nano and micro-structure with a scanning electron microscope (SEM) and performing chemical analysis using thermogravimetric analysis (TGA). Mechanical property such as modulus of rupture (flexural strength) was measured using an Instron universal testing machine and a water resistance study was conducted using a tensiometer to measure contact angle and surface water absorption. SEM images showed wood lumens thickened and collapsed, with a filled-in sub-structure, leading to a compact multi-layered assembly. The functionalized densified material had better surface wear resistance and excellent mechanical performance (flexural strength was approximately 150% higher than that of the original wood and surface hardness was enhanced). The water absorption rate of the functionalized densified samples reduced significantly compared to the original wood which in turn enhanced the surface water repellency. This was due to the reduction of hydrophilic groups as well as the clogging of the pores (pits) on the wood surface. Such enhanced performance makes the functionalized densified wood composite a promising candidate for advanced structural and engineering applications.

Received 14th August 2023,  
Accepted 17th October 2023

DOI: 10.1039/d3ma00550j

rsc.li/materials-advances

## Introduction

Wood has been used in construction and structural application because of its good aesthetics and mechanical properties.<sup>1</sup> Moreover, utilizing wood instead of fossil fuel-based materials also contributes to maintaining the carbon cycle balance as wood stores carbon dioxide.<sup>2</sup> However, wood has certain drawbacks such as high sensitivity to moisture, and infestation of microorganisms in addition to the high anisotropic nature limits the usability of wood for advanced engineering structures and applications. In order to enhance the mechanical performance, improve surface water resistance and modify the wood to reduce the high variability, wood-based advanced bioproducts have been developed.<sup>1</sup>

Wood can generally be modified *via* chemical, thermal, or mechanical methods.<sup>3</sup> One of the simplest and most prominent mechanical methods to increase the structural properties of wood is through the densification process.<sup>3–6</sup> Densified

wood products with increased density can be a substitute for other structural materials because of enhanced hardness and mechanical performance. Previous studies have shown that the densification process makes it possible to manufacture moisture resistance, high-density wood from commercially available low-density medium-rotation wood species (*e.g.*, hybrid aspen).<sup>7,8</sup> It has been reported that pre-treatment on advanced wood products such as steam, ammonia, and heat<sup>9–18</sup> followed by a densification process can improve the mechanical performance of natural wood. However, the wood treated with these methods resulted in an incomplete densified wood product which expanded and weakened in the presence of moisture and hence lacked dimensional stability, especially in a humid environment.<sup>14</sup> To overcome this challenge and to ensure complete densification a simple but effective process of transforming bulk wood into high-performance structural material (10× increase in strength, toughness, and ballistic resistance and with greater dimensional stability) has been reported by Song *et al.*<sup>19</sup> The process includes two steps involving partial removal of lignin and hemicellulose *via* alkaline treatment followed by hot pressing for a day. The delignification is done to aid the mechanical densification process.<sup>20–23</sup> The processed wood has a specific strength much higher than some structural alloys and metals.<sup>19</sup> Although densification yields wood products with high strength, it consumes a

<sup>a</sup> Chemical and Biological Engineering, University of British Columbia, Vancouver, Canada. E-mail: johan.foster@ubc.ca

<sup>b</sup> Hugh Boyd Highschool, 9200 No. 1 Rd. Richmond, British Columbia, Canada

† Electronic supplementary information (ESI) available. See DOI: <https://doi.org/10.1039/d3ma00550j>



lot of time (12–24 hours for densification) and energy to compress the wood to ensure it from bouncing back.<sup>24–26</sup> Additionally, we need to use extra chemicals *e.g.* polyurethane<sup>19</sup> to coat the surface in order to prevent it from moisture and micro-organisms attack.

Previously wood fibres have also been used in combination with thermoset resins to produce panels with excellent properties compared to the original wood. In the work done by Wei *et al.*<sup>27</sup> densified laminated material was manufactured using wood fibre mats impregnated with phenolic resin. The densified product had favourable water resistance and enhanced mechanical properties compared to the original wood.<sup>27</sup> However, in applications where the original natural form of wood is required, especially in the outdoors, various treatments have been employed to modify wood.<sup>27</sup> For instance, resin impregnation in cellular walls or lumens, surface coatings using various chemicals, and heat-induced *in situ* polymerization are the common ways to chemically modify wood.<sup>28–31</sup>

Chemical modification of wood can also be attained *via* reacting hydroxyl groups of wood with isocyanates/epoxides or through the esterification of hydroxyl groups using acid anhydrides to attain hydrophobicity.<sup>32–36</sup> To improve the anti-swelling efficiency of wood, lumen filling has been done using various petrochemical polymers such as formaldehyde resin,<sup>37</sup> methyl methacrylate,<sup>38</sup> and polyethylene glycol.<sup>39</sup> However, these special chemicals for wood property enhancement are harmful to the environment while manufacturing or towards the end of the product life cycle.<sup>1</sup> Hence, environmental concern has led to the manufacturing of biobased wood products using benign renewable chemicals which are easily compostable or degradable.

Poly(lactic acid) (PLA) is a plant-based biodegradable thermoplastic polymer, which is a sustainable and environmentally friendly alternative to petroleum-based polymers.<sup>40</sup> Moreover, using biobased resources reduces dependency on fossil fuels and also provides a solution to eco-friendly concerns.<sup>22,41</sup> From a chemistry point of view, PLA is produced from the polycondensation reaction between hydroxyl groups and carboxylic acid groups of lactic acid monomers.<sup>42</sup> And *via* the removal of water produced as a by-product during condensation reaction, the overall reaction moves in the forward direction to produce PLA.<sup>42</sup> PLA has several desirable properties such as high strength, high modulus, good grease, and oil resistance.<sup>43–47</sup> It has been extensively used in combination with natural fibres such as jute, flax, and hemp to produce compressed or extruded composite materials with good environmental characteristics and better mechanical properties.<sup>48–53</sup> Moreover, previous literature has shown that PLA has a higher affinity toward natural cellulosic fibres compared to hydrophobic polymers such as polyvinylchloride, polypropylene, and polyethylene.<sup>49</sup> In the work done by Noël *et al.*<sup>1</sup> lactic acid-infused wood composite was made with different physical properties for flooring and indoor applications. The developed composite showed to have better biological resistance and mechanical properties compared to the original wood sample.<sup>1</sup> However, the samples require extensive heating cycles to produce.<sup>1</sup>

The current work combines two separate techniques of wood modification *i.e.*, lumen filling (chemical modification) and

densification (mechanical modification) to produce the advanced bio-products in a single step of *in situ* polymerization and densification.<sup>54</sup> To the best of our knowledge, this method of combining the densification with the chemical modification using biobased polymer (polylactic acid) has not been reported. This technique is an environmentally friendly and effective method to enhance wood performance. Our hypothesis is that the lactic acid oligomers will get grafted in the cellulosic structure filling up the voids, and pits, to give better water repellency properties to the composite. Moreover, while we densify the same oligomers also act as a reactive agent which will bond (hydrogen/covalent) with the hydroxy group of cellulose and expedite the densification process to save time and energy. The structure, mechanical performance, and water resistance of the final densified material were investigated. The objective of this study was to develop an industrially feasible strategy requiring less time and energy for the preparation of high-performance densified wood material.

## Materials and methods

### Materials

L-(+)-Lactic acid 80, which is an 80% aqueous solution of the monomer, sodium hydroxide for the delignification process was purchased from Sigma-Aldrich. Cedar wood samples (5.45 × 37.5 × 100 mm<sup>3</sup>, transverse × radial × longitudinal oriented) were cut from the cedar tree and were purchased from the local Home Depot. Deionized water was used. Douglas Fir, Maple, Birch, Aspen, Spruce, and Balsam were obtained directly from British Columbia's forests.

### Wood delignification

First, natural wood blocks (dimension: 100.0 mm by 5.45 mm by 37.5 mm) were treated with an aqueous solution of 2.5 M NaOH for 7 h at 80 °C. Then the treated samples (termed delignified wood) were immersed and washed with deionized water multiple times till the pH of washed water dropped to approximately 7 ensuring the removal of the chemicals. Next, the delignified wood blocks were frozen and then freeze-dried using benchtop freeze dryers by Labconco to remove the water for further treatment.

### Lactic acid oligomers synthesis

To prepare lactic acid oligomers (LAO), 80% aqueous solution of L-(+)-lactic acid was dehydrated, and then polycondensation of lactic acid was carried out without any catalyst. Polymerization was done under vacuum using a Heidolph rotary evaporator equipped with an oil bath to reach a temperature above 100 °C. The round bottom flask was heated to 120 °C under vacuum (30 mmHg) and the polymerization was carried out for 1 h once ebullition stopped. After 1 h, the molten viscous lactic acid oligomers, referred to as lactic acid oligomer (LAO), was stored in a closed flask at ambient temperature.

### LAO-wood polymerized-densified composite synthesis

To prepare LAO-wood *in situ* polymerized-densified samples, the original (natural wood), as well as delignified wood



samples, were oven-dried at 103 °C until a constant weight was achieved and then submerged into LAO. The system (wood + LAO) was placed into a vacuum desiccator and then exposed to two alternative vacuum and atmospheric pressure cycles of 2 hours each. Impregnated wood samples were then carefully removed and dabbed with tissue to remove excess LAO. Then the impregnated samples were introduced to densification and heating to further polymerize at 120 °C in a hot-press carver for 1 h at 5 MPa, followed by oven curing at 105 °C for 24 hours. Schematic of the process is shown in Fig. 1(A). On the other hand, some samples (LAO impregnated original as well as delignified) were just introduced to a heating cycle of 1 hour at 120 °C without densification and then cured in a ventilated oven at 105 °C for 24 hours to understand the effect of densification. Some samples (original as well as delignified) were just densified (120 °C, 5 MPa) without impregnating LAO in the wood to compare the effect of LAO on the final LAO-wood *in situ* polymerized densified composite.

### Experimental design

There were 8 different samples prepared including the control (original wood). The wood blocks were randomly assigned to these 8 different treatments. Fig. 1(B) shows the various treatment carried out on the original wood. Every treatment had at least 5 replicates. In the previous literature, densification has already been done, and similarly, research on lactic acid impregnation and just curing has also been done. But our study combines both studies to counter the obstacle of extensive treatment time in

densification as well as modifying wood to improve the water sensitivity of the final wood composite in just one step. The original wood was our control sample and went to 3 different treatments. (1) Densification (OD): indicates that the original wood was directly densified; (2) functionalized cured (OFC): indicated LAO was impregnated in the original wood and *in situ* polymerization was carried out; (3) functionalized densified (OFD): LAO was impregnated in the original wood and *in situ* functionalization densification was carried out. Similar treatments were carried out after delignification also. The delignified sample (D) and the nomenclature used for delignified densified, delignified functionalized cured, and delignified followed by *in situ* functionalization densification were DD, DFC, and DFD, respectively. A total of 8 different treatments were investigated.

### Liquid chromatography–mass spectroscopy (LC–MS)

Molecular weight analysis of LAO was done on Bruker HCT, a high-capacity ion trap mass spectrometer equipped with an electrospray (ESI) ion source. An injection volume of 5  $\mu\text{L}$  was introduced under ambient temperature using flow injection at 0.2 ml  $\text{min}^{-1}$ . Agilent 1100 HPLC was coupled for the LC–MS analysis with 100% acetonitrile as the mobile phase. The Bruker Compass Data Analysis 4.0 was used for data acquisition and processing.

### Attenuated total reflectance-Fourier transform infrared spectroscopy (ATR-FTIR) analysis

FTIR spectra for wood and composite were recorded on a Bruker Inventio ATR-FTIR spectrometer. Finely divided sawdust was carefully spread on the diamond crystal and adequate pressure was applied to ensure there was no air present between the crystal and the samples. For the liquid samples (lactic acid and lactic acid oligomers) a drop was poured on the crystal making sure it covers the whole crystal surface and no pressure was applied. The spectra were recorded in the range of 4000–400  $\text{cm}^{-1}$  with a resolution of 4  $\text{cm}^{-1}$  by averaging 32 scans.

### Scanning electron microscopy (SEM) analysis

Scanning electron microscopy was performed on a Hitachi SU3500 apparatus. Sample surfaces were sputter-coated with iridium (8–9 nm coating thickness) using Leica EM MED020 Coating. The accelerating voltage of 1 kV was used for imaging.

### Contact angle and water absorption test

Theta Flex 300-pulsating drop 200 Tensiometer was used to calculate static contact angle and water absorption on the wood surface. The droplet size was 5–10  $\mu\text{L}$ . After releasing the droplet, the contact angle and the water absorption were observed for 60 seconds.

### Mechanical testing – modulus of rupture (MOR)

The specimens were loaded at the center of the span with the load applied to the top surface of the specimen. Testing was done at a uniform loading rate of 10 mm  $\text{min}^{-1}$ . A universal testing machine from Instron was used to carry out the 3-point bending test (ASTM D4761-19) with modification.<sup>55</sup> The sample length span was set to 90 mm.

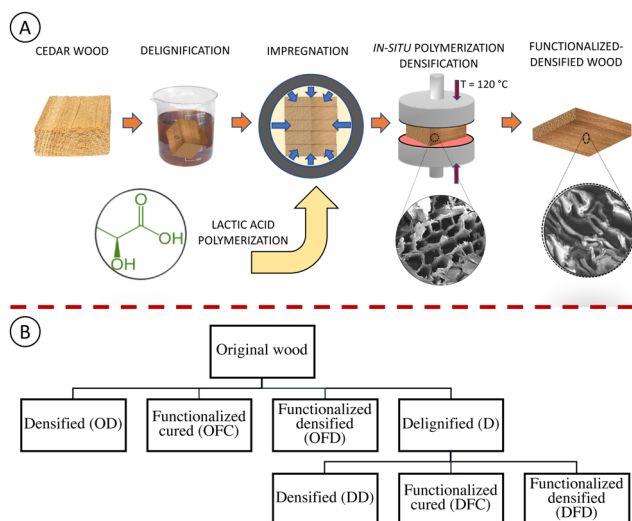


**Fig. 1** (A) Schematic for the synthesis of *in situ* functionalized densified (DFD) wood composite. Natural wood was partially delignified using alkaline solution (NaOH) followed by the vacuum impregnation of polymerized lactic acid (LAO). Then the impregnated samples went through *in situ* polymerization and densification process to finally get the functionalized densified wood composite. (B) Experimental design showing the 8 different treatments done on the natural wood. Although the main highlight of the study was *in situ* functionalized densified wood (DFD), to compare the effect of densification, LAO impregnation, and polymerization separately on original as well as delignified wood, OFC, OFD, DD, DFC were manufactured. Mechanical properties (MOR) for 8 different treatments were compared to see the treatment effect.



## Thermogravimetric analysis (TGA)

Thermogravimetric (TG) curves for original wood and *in situ* functionalized densified wood composite were recorded using a thermogravimetric analyzer TGA 5500. Samples (5–10 mg) were heated under a nitrogen atmosphere from 25 to 700 °C at a heating ramp of 20 °C min<sup>-1</sup>. Derivative thermogravimetric curves (DTG) were obtained from TG curve data which displays the weight loss rate as a function of temperature.

## Results and discussion

### LAO molecular weight characterization LC-MS results

In the current study, LAO was manufactured *via* direct melt polycondensation reaction without any catalyst, as reported by Noël *et al.*<sup>1</sup> To ensure good impregnation in the wood lumens, LAO should have low viscosity and a small degree of polymerization. In our study, LAO was prepared by condensation of lactic acid under vacuum at 120 °C, and qualitatively analyzed by liquid chromatography–mass spectroscopy (LC-MS) shown in Fig. S1 (ESI<sup>†</sup>), and Table S1 (ESI<sup>†</sup>). We observed that the lactic acid oligomers' retention time was between 1.1–1.7 min from the total ion chromatogram obtained *via* LC-MS analysis Fig. S1 (ESI<sup>†</sup>). It was evident that catalyst-free polycondensation yielded the oligomers with a higher degree of polymerization ranging from 3-mer to 8-mer, with a peak intensity at the 5-mer.

### LAO characterization: ATR-FTIR

Further confirmation of polycondensation groups was carried out using ATR-FTIR (Fig. 2). Fig. 2 shows the full ATR-FTIR spectra (on left) for lactic acid (solid blue line) as well as lactic

acid oligomers (graph in dotted orange line) and a zoomed section (ranging from 1500–700 cm<sup>-1</sup>) of the spectra comparing lactic acid and LAO. It was observed that the generated LAO had characteristic bands at 760 cm<sup>-1</sup>, 875 cm<sup>-1</sup>, 1390 cm<sup>-1</sup>, and 1460 cm<sup>-1</sup> which corresponds to  $\delta(\text{C}=\text{O})$ ,  $\gamma(\text{C}-\text{COO})$ ,  $\delta\text{s}(\text{CH}_3)$ , and  $\delta\text{as}(\text{CH}_3)$ , respectively which have been reported in the previous literature confirming successful polycondensation of the lactic acid.<sup>1,56,57</sup> Moreover, the carbonyl (C=O) stretching band of lactic acid, corresponding to the acid groups from monomers, showed a band at 1720 cm<sup>-1</sup> which was broad compared to the (C=O) stretching for LAO. In the case of LAO, the (C=O) stretching band was narrow and appeared between 1740 and 1750 cm<sup>-1</sup> corresponding to aliphatic esters this trend has been seen in previous work<sup>57–60</sup> confirming the successful polymerization of lactic acid. Additionally, the spectra of LAO showed weak band attributing to hydroxyl groups around 3500 cm<sup>-1</sup>, due to polycondensation reaction (LCMS analysis Fig. S1, ESI<sup>†</sup>) leading to less hydroxyl groups present.<sup>57</sup>

### Wood-based composite characterization: SEM analysis

After the preparation and characterization of LAO, it was impregnated into delignified wood (D). The LAO-impregnated delignified wood was then *in situ* polymerized and densified (DFD). To understand the effect of LAO grafting and polymerization on the cell walls of wood composite SEM images of the cross-section were observed and are reported in Fig. 3(D–I). It was evident from Fig. 3 that the original wood had open wood channels 'lumina' a honeycomb-like structure (Fig. 3D, and G). After the densification, the cell walls collapsed (Fig. 3E, and H). It was interesting to see that wood after *in situ* functionalization and densification had thicker cell walls indicating the grafting

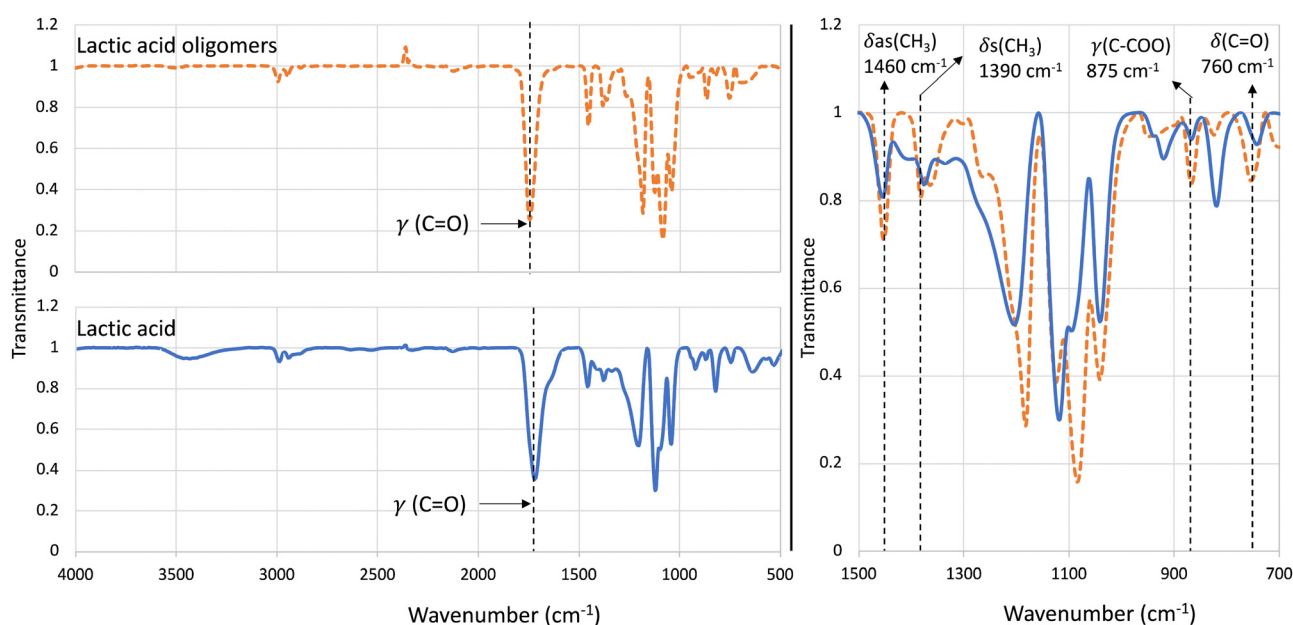
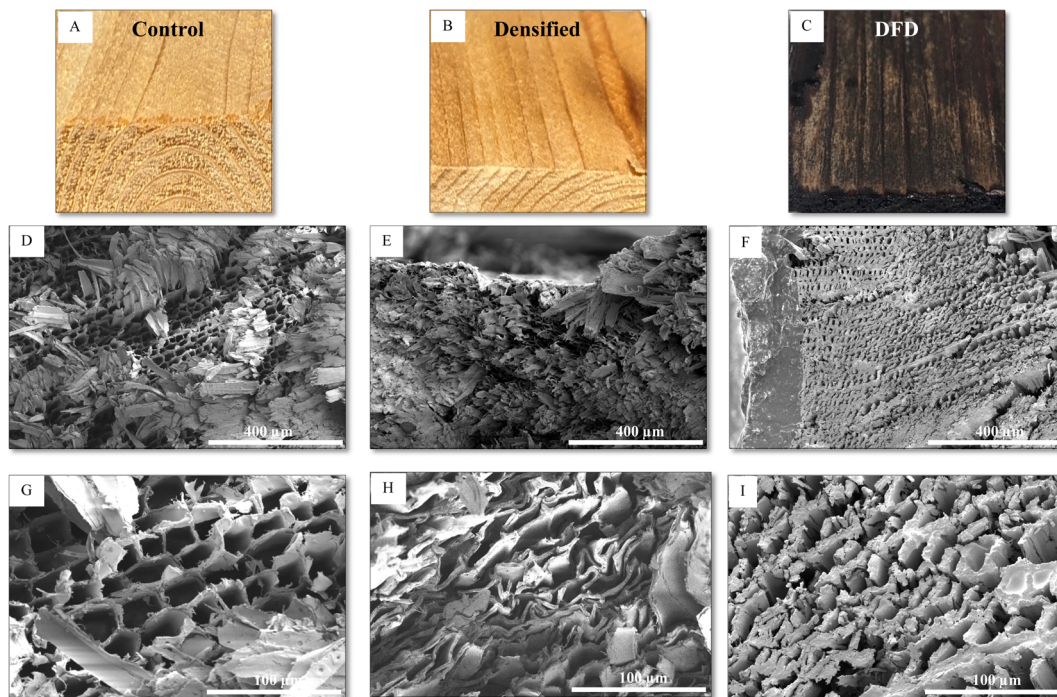


Fig. 2 (left) ATR-FTIR spectra of lactic acid oligomers (dotted orange line), lactic acid (solid blue). (right) Zoom ATR-FTIR spectra from 1500–700 wavenumber. Black vertical dotted lines show the key spectral bands used to monitor the polymerization reaction. The characteristics bands because of polymerization reaction, are associated with increase of intensity for  $\gamma(\text{C}=\text{O})$  – 1750–1720 cm<sup>-1</sup>,  $\delta\text{as}(\text{CH}_3)$  – 1460 cm<sup>-1</sup>,  $\delta\text{s}(\text{CH}_3)$  – 1390 cm<sup>-1</sup>,  $\gamma(\text{C}-\text{COO})$  – 875 cm<sup>-1</sup>,  $\delta(\text{C}=\text{O})$  – 760 cm<sup>-1</sup>,  $\gamma$ : stretching,  $\delta$ : bending, as: anti symmetric, s: symmetric.





**Fig. 3** Images of actual sample (A) control, (B) delignified densified, and (C) DFD (delignified and *in situ* functionalized densified). SEM images of cross-sectional morphology (D), (E) and (F) show the magnified image (HFW\*: 1 mm) for the original, delignified densified, and the DFD samples respectively; SEM images (G), (H) and (I) show the magnified image (HFW\*: 250  $\mu\text{m}$ ) for the original, delignified densified, and the DFD samples respectively. \*Horizontal field width.

of LAO to the cell walls and in this treatment, the cell walls also collapsed (Fig. 3F and I)

### TGA analysis

To confirm our visual observation that LAO was getting impregnated and polymerized in the wood lumens thermogravimetric

analysis (TGA) of original and *in situ* polymerized densified wood (DFD) (Fig. 4) was done. In the case of original/untreated wood, we observed a characteristic temperature degradation profile (Fig. 4). Initially, below 50  $^{\circ}\text{C}$  to 125  $^{\circ}\text{C}$ , water loss was observed, and it was not until 200  $^{\circ}\text{C}$  when wood degradation processes became more evident (Fig. 4 – deriv. original). Firstly weight loss was due to the decomposition of extractives<sup>61,62</sup>

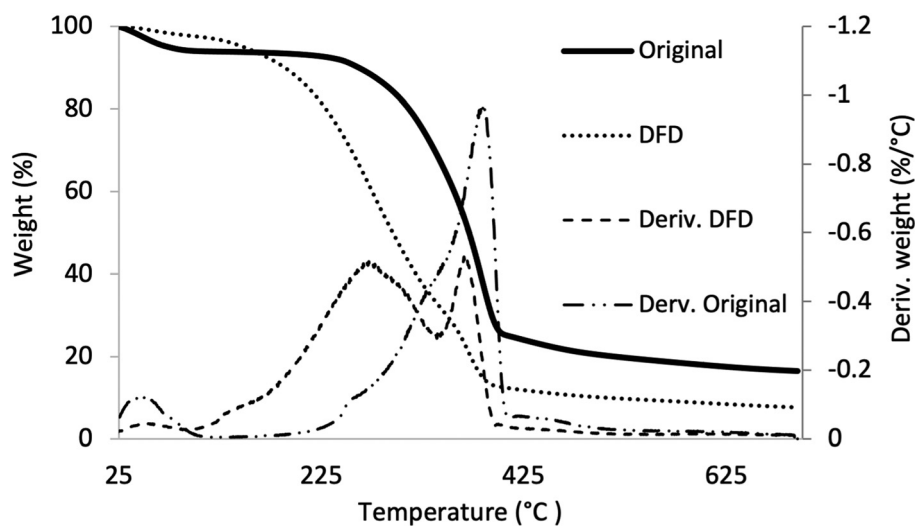


**Fig. 4** Thermogravimetric/derivative thermogravimetric (TG/DTG) curves of original wood (untreated), *in situ* functionalized densified wood (DFD); deriv: derivative TG curve. The derivative curve for DFD sample shows an extra peak (100–300  $^{\circ}\text{C}$ ) corresponding to the degradation of polymerized LAO which was not visible for the original wood.



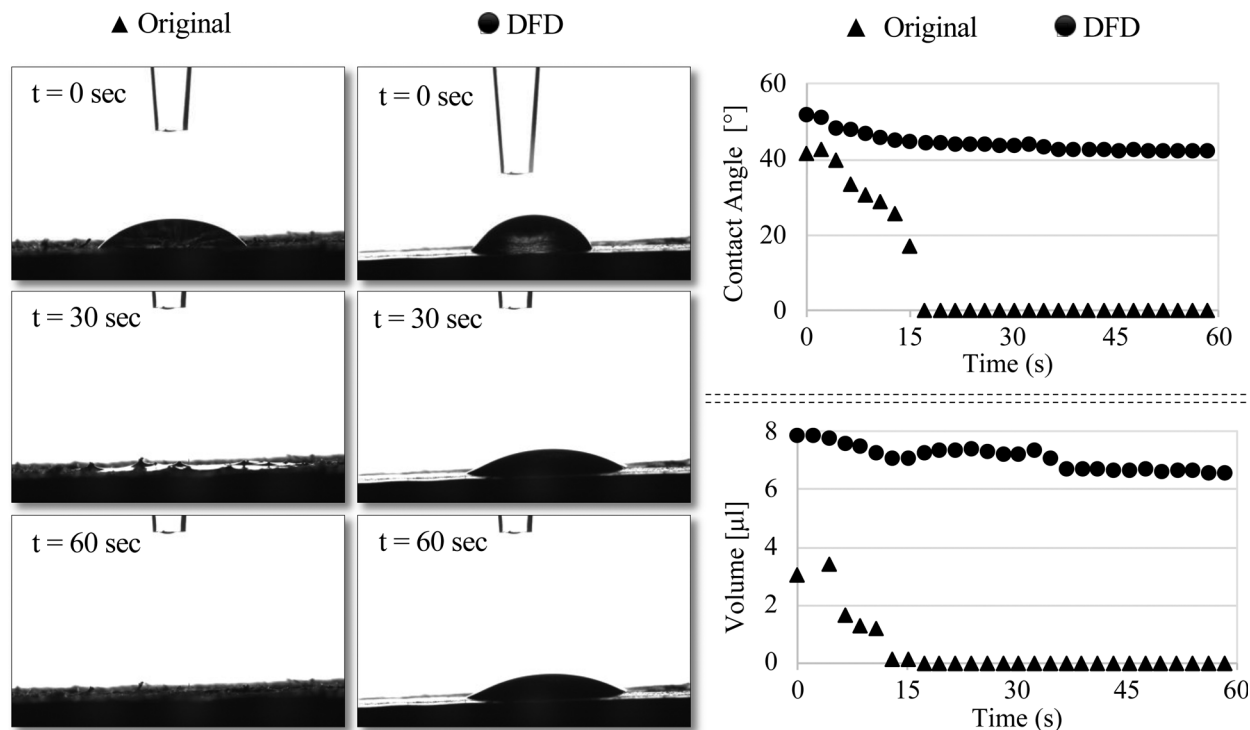


**Fig. 5** Static sessile drop test for original ( $\blacktriangle$ ) and DFD (delignified and *in situ* functionalized densified – ( $\bullet$ )) wood composites ( $t$ : time). The image on the left shows the interaction of water droplet on the original as well as the DFD sample surface. After  $t = 60$  seconds the water droplet was completely absorbed by the original wood surface. On the contrary, at  $t = 60$  seconds the DFD sample still had water droplet on the surface showcasing better water repellency property. Results on the right show graphs for contact angle vs. time and volume of absorbed water vs. time. Contact angle for the original sample dropped from  $41^\circ$  ( $t = 0$  s) to  $0^\circ$  ( $t = 15$  s) and was not measurable after 15 seconds whereas the contact angle for the DFD sample decreased a little from  $52^\circ$  to  $43^\circ$  but remain constant after 15 seconds. The water absorption graph on the bottom right shows the water droplet getting completely absorbed on the original sample surface after 15 seconds whereas for the DFD sample the water absorption was very low.

followed by hemicellulose degradation above  $285^\circ\text{C}$ .<sup>63</sup> Below  $350^\circ\text{C}$ , cellulose started to depolymerize,<sup>64–66</sup> and above  $390^\circ\text{C}$  decomposition of lignin occurred.<sup>67–69</sup> The differential thermogravimetric analysis (deriv.) curve of the DFD (Fig. 4) sample comprised two peaks. The broad peak between  $100$ – $340^\circ\text{C}$  was because of the degradation of polymerized LAO. Moreover, this broad peak is contributed not only by the decomposition of polymerized LAO, present in DFD, but also by water loss from further polycondensation.<sup>57,70</sup> The second peak corresponded to the cellulose degradation like the original sample. It was evident

from TGA and DTG curves that LAO was polymerized into the wood lumens and getting adhered to the wood.

#### Contact angle and water absorption

LAO was used as a bio-based polymer to strengthen the densified wood and to prevent the wood from absorbing water once it is polymerized into the wood lumens as well as on the surface. To understand the water repellency property of the final composite sessile drop test was performed on the surface. Contact angle and water absorption measurement indicated that water absorption

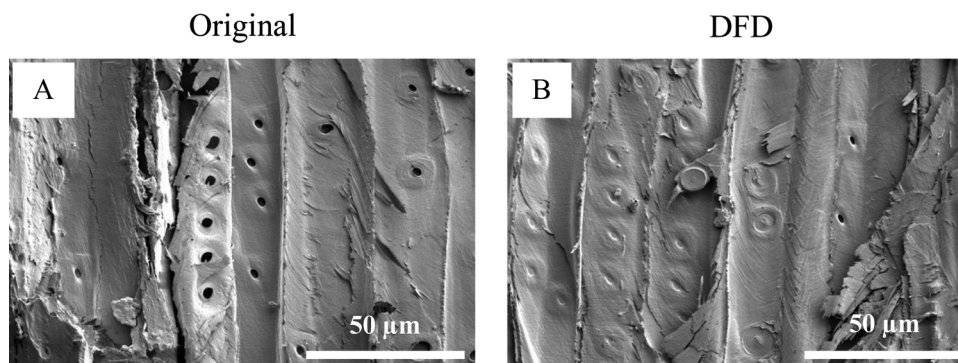


**Fig. 6** SEM images of the original wood and DFD surface showing the open pores (pits) 'A' and closed/clogged pits 'B'. Open pores allow the transfer of minerals and water to the adjacent cell wall. Closing them by blocking or filling up with polymers improves the water repellency property of wood.



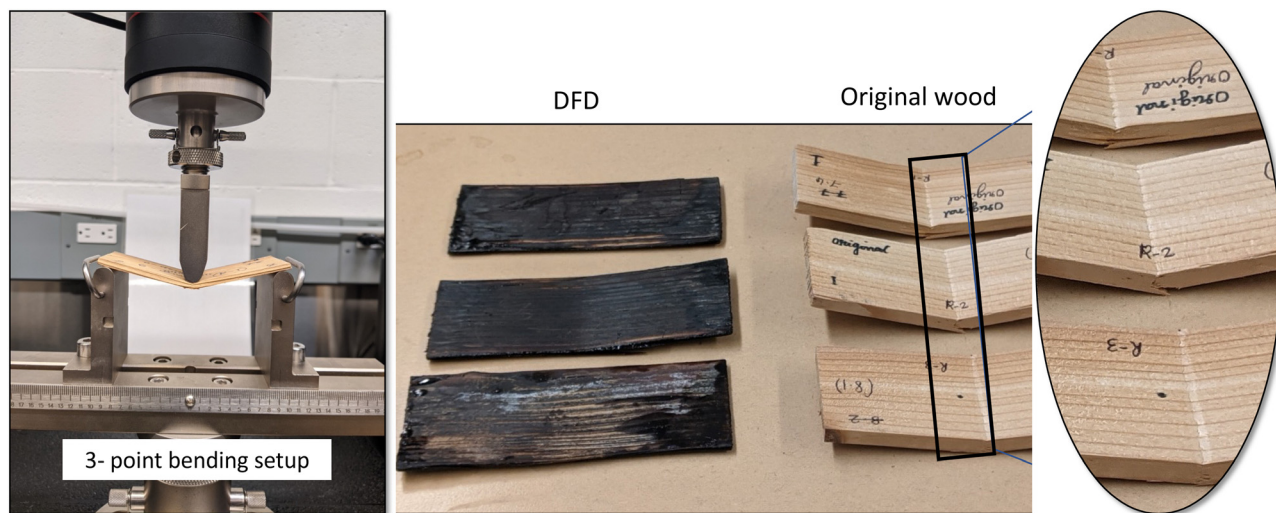


Fig. 7 (left) 3-point bending setup and (right) qualitative hardness testing using 3-point bending test showing severe indentation on the original wood surface compared to DFD surface, (DFD samples had better surface hardness)

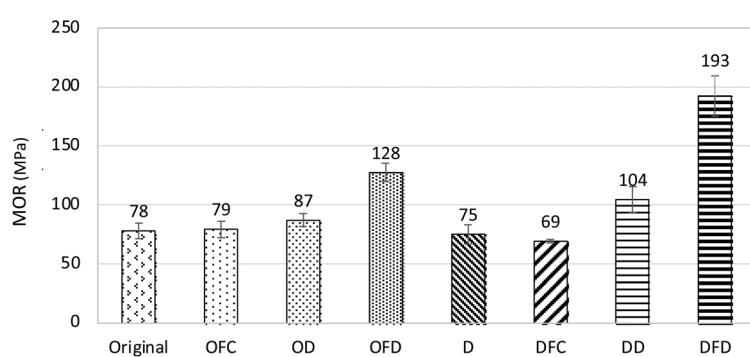
was significantly high in the original wood compared to the functionalized densified wood (DFD) Fig. 5. The contact angle for the original sample decreased from  $41^\circ$  to  $0^\circ$  in just 15 seconds to its contrary for the DFD sample it decreased from  $52^\circ$  to  $43^\circ$ . Similarly, the volume of a water droplet was reduced to  $0 \mu\text{L}$  in the original sample after 15 seconds, whereas the volume of a water droplet on the DFD surface was reduced from  $8 \mu\text{L}$  to  $7 \mu\text{L}$  after 15 seconds. The main reason for the decrease in water absorption for DFD is due to the collapse of pores (pits) present on the surface of wood, as shown in SEM images (Fig. 6). Moreover, the cross-sectional SEM images (Fig. 3F and I) showed that the LAO was getting polymerized and adhering to the cell walls blocking up the void (pits). So, biobased LAO impregnation eventually improves the sensitivity of wood-based products against moisture preventing the densified wood from swelling/bouncing back, which was the main gap in previous literature.<sup>14</sup>

### Modulus of rupture (MOR) and hardness

All samples went through a three-point bending test to measure the Modulus of Rupture (MOR) using Instron. Before calculating

MOR, the hardness of the original and functionalized densified wood was qualitatively assessed. It was evident from Fig. 7 that the indentation caused after the three-point bending test on the original wood sample had significant depth compared to the functionalized densified sample. The 3-point bend test was run till the samples yielded. Modulus of Rupture (MOR) for 8 different treatments was calculated and are shown in Fig. 8. Compared to original wood samples MOR increased by  $\sim 150\%$  for the delignified *in situ* functionalized densified (DFD) samples. This is because of the polymerization of lactic acid oligomers between cell walls plus the formation of hydrogen bonding among the adjacent cell walls during densification. These two phenomena led to increasing in the strength of the final product.

Similarly, there was an increase in the MOR for the original *in situ* functionalized densified (OFD) samples as well. But the extent of increment was not as significant as DFD. This is because the delignification step in DFD partially removes the lignin and hemicellulose from the wood samples which creates extra spaces/pores in the wood. And the removal of lignin makes it easier to densify the wood which creates more



Samples	MOR (MPa)
Original (ORG)	$78 \pm 7$
Original Functionalized Cured (OFC)	$79 \pm 6$
Original Densified (OD)	$87 \pm 6$
Original Functionalized Densified (OFD)	$128 \pm 8$
Delignified (D)	$75 \pm 8$
Delignified Functionalized Cured (DFC)	$69 \pm 3$
Delignified Densified (DD)	$104 \pm 11$
Delignified Functionalized Densified (DFD)	$193 \pm 17$

Fig. 8 Modulus of rupture (graph and table) for 8 different treatments; highest MOR was recorded for the DFD samples and the lowest for the delignified samples. Abbreviations – Org: original; OFC: original functionalized cured; OD: original densified; OFD: original functionalized densified; D: delignified; DFC: delignified functionalized cured; DD: delignified densified; DFD: delignified *in situ* functionalized densified.



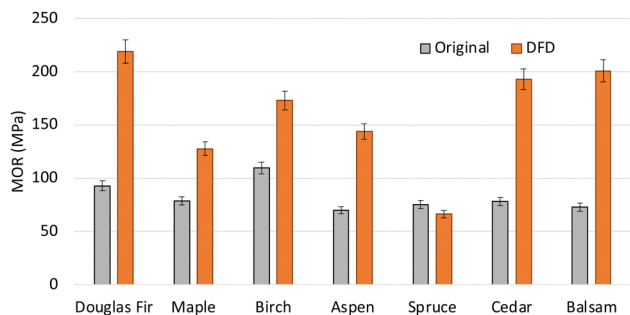


Fig. 9 MOR study conducted on other species found around British Columbia (BC): Douglas Fir, Maple, Birch, Spruce, and Balsam. A similar strategy as mentioned in the paper for DFD preparations was employed on these samples and MOR was recorded. All the samples were delignified, followed by impregnation and *in situ* polymerisation densification.

opportunities to form hydrogen bonding between the adjacent cell walls.<sup>20–23</sup> Moreover, due to the formation of pores in the wood, the uptake of polymer also increases which results in better void filling and more polymerization products.

The previous study has proven that partial removal of lignin (~50%) has led to an increase in the strength of densified wood compared to the original.<sup>19</sup> Similar trend in MOR was observed in our study also. Delignified densified samples (DD) had more strength than the original as well as delignified samples (D). To compare the effect of just LAO impregnation and polymerization with respect to DFD, original samples, as well as delignified samples, were impregnated and cured without densifying. It was observed that LAO polymerization did not increase MOR in the case of OFC (79 MPa) and DFC (69 MPa) compared to the original wood (78 MPa). However, polymerization combined with densification boosted the MOR for OFD (128 MPa) as well as DFD (193 MPa). It was very well evident in the SEM images (Fig. 3F and I) also that the polymerization of LAO oligomers assisted in providing extra strength by keeping the cell wall intact by acting as a glue. To broaden the applicability of the process, six different species were subjected to an *in situ* functionalization densification process (Fig. 9). It was observed that in all the cases except spruce, the DFD samples had higher MOR compared to the original wood sample.

## Conclusions

This work has demonstrated a promising association between two environmentally friendly resources wood and polylactic acid. We investigated the process to densify wood along with *in situ* polymerization using biobased polymer to develop mechanically stronger as well as functionalized wood composite. MOR of the delignified functionalized densified wood improved significantly compared to the original wood sample, delignified densified (DD) samples as well as delignified functionalized cured (DFC) samples. This shows the synergistic effect of simultaneous LAO polymerization with the densification process. Moreover, the advantage of using biobased polymer was also evident from the performance improvement of

wood composite against water which was measured through the sessile water droplet test. The qualitative hardness of the DFD samples was also enhanced compared to the original wood. This strategy of simultaneous densification along with polymerization requires less time and energy to densify compared to the traditional densification process. Moreover, the use of biobased polymers makes the process more environmentally friendly. The future work will be focused on optimizing the process for other species of wood to develop wood-based composites for advanced engineering applications.

## Author contributions

Akash Gondaliya: conceptualization, methodology, experiments, data analysis, writing the original draft; Kieran Foster: resource; E. Johan Foster: supervision, conceptualization, review and editing, funding acquisition.

## Conflicts of interest

There are no conflicts to declare.

## Acknowledgements

This work was supported by the NSERC Canfor Industrial Research Chair in Advanced Bioproducts. SEM was performed in the Centre for High-Throughput Phenogenomics at the University of British Columbia, a facility supported by the Canada Foundation for Innovation, the British Columbia Knowledge Development Foundation, and the UBC Faculty of Dentistry. The hot-press facility was performed by Prof. Savvas's Lab, and Prof. Feng Jiang's Lab. FTIR-ATR was performed at Prof. Scott Rennecker's lab. Dept of Wood Science UBC (Lief Eriksen, Claudia Ediger), Mass spectrometry research facility (Dept of Chemistry, UBC)

## Notes and references

- 1 M. Noël, E. Fredon, E. Mougél, D. Masson, E. Masson and L. Delmotte, *Bioresour. Technol.*, 2009, **100**, 4711–4716.
- 2 C. Dearing Oliver, N. T. Nassar, B. R. Lippke and J. B. McCarter, *J. Sustainable For.*, 2014, **33**, 248–275.
- 3 D. Sandberg, A. Kutnar and G. Mantanis, *IForest*, 2017, **10**, 895–908.
- 4 A. Kutnar and M. Šernek, *Zb. gozdarstva Lesar.*, 2007, 53–62.
- 5 M. Kadivar, C. Gauss, K. Ghavami and H. Savastano, *Materials*, 2020, **13**, 1–25.
- 6 J. P. Cabral, B. Kafle, M. Subhani, J. Reiner and M. Ashraf, *J. Wood Sci.*, 2022, **68**, 20.
- 7 J. Blomberg and B. Persson, *J. Wood Sci.*, 2004, **50**, 307–314.
- 8 J. Blomberg, B. Persson and A. Blomberg, *Wood Sci. Technol.*, 2005, **39**, 339–350.
- 9 A. Kutnar, F. A. Kamke, A. Kutnar and F. A. Kamke, *Wood Sci. Technol.*, 2012, **46**, 73–88.





- 10 C. A. S. Hill, J. Ramsay, B. Keating, K. Laine, L. Rautkari, M. Hughes and B. Constant, DOI: [10.1007/s10853-011-6154-8](https://doi.org/10.1007/s10853-011-6154-8).
- 11 K. Laine, T. Belt, L. Rautkari, J. Ramsay, C. A. S. Hill and M. Hughes, *J. Mater. Sci.*, 2013, **48**, 8530–8538.
- 12 C.-H. Fang, N. Mariotti, A. Cloutier, A. Koubaa, P. Blanchet, A. Cloutier, P. Blanchet and A. Koubaa, *J. Wood Prod.*, 2012, **70**, 155–163.
- 13 P. Bekhta, S. Hiziroglu and O. Shepelyuk, *Mater. Des.*, 2009, **30**, 947–953.
- 14 P. Pařil, M. Brabec, O. Maňák, R. Rousek, P. Rademacher, P. Čermák and A. Dejmal, *Eur. J. Wood Wood Prod.*, 2014, **72**, 583–591.
- 15 P. Navi and F. Heger, *MRS Bull.*, 2004, **29**, 332–336.
- 16 M. Gong, C. Lamason and L. Li, *J. Mater. Process. Technol.*, 2010, **210**, 293–296.
- 17 K. Laine, K. Segerholm, M. Wälinder, L. Rautkari and M. Hughes, *Wood Sci. Technol.*, 2016, **50**, 883–894.
- 18 Y. Luan, C. H. Fang, Y. F. Ma and B. H. Fei, *Mater. Manuf. Process.*, 2022, **37**, 359–371.
- 19 J. Song, C. Chen, S. Zhu, M. Zhu, J. Dai, U. Ray, Y. Li, Y. Kuang, Y. Li, N. Quispe, Y. Yao, A. Gong, U. H. Leiste, H. A. Bruck, J. Y. Zhu, A. Vellore, H. Li, M. L. Minus, Z. Jia, A. Martini, T. Li and L. Hu, *Nature*, 2018, **554**, 224–228.
- 20 Y. Ran, D. Lu, J. Jiang, Y. Huang, W. Wang and J. Cao, *Chem. Eng. J.*, 2023, **471**, 144476.
- 21 Y. Chen, B. Dang, C. Jin and Q. Sun, *ACS Nano*, 2019, **13**, 371–376.
- 22 H. Luo, R. Si, J. Liu, P. Li, Y. Tao, X. Zhao and H. Chen, *Cellulose*, 2022, **29**, 7377–7396.
- 23 A. Kumar, T. Jyske and M. Petrič, *Adv. Sustainable Syst.*, 2021, **5**, 2000251.
- 24 J. Shi, J. Peng, Q. Huang, L. Cai and S. Q. Shi, *J. Wood Sci.*, 2020, **66**, 5.
- 25 Z. Fan, H. Sun, L. Zhang, X. Zhao and Y. Hu, *ACS Sustainable Chem. Eng.*, 2022, **10**, 9600–9611.
- 26 J. Song, C. Chen, S. Zhu, M. Zhu, J. Dai, U. Ray, Y. Li, Y. Kuang, Y. Li, N. Quispe, Y. Yao, A. Gong, U. H. Leiste, H. A. Bruck, J. Y. Zhu, A. Vellore, H. Li, M. L. Minus, Z. Jia, A. Martini, T. Li and L. Hu, *Nature*, 2018, **554**, 224–228.
- 27 J. Wei, F. Rao, Y. Zhang, W. Yu, C. Hse and T. Shupe, *Mater. Lett.*, 2019, **253**, 358–361.
- 28 S. S. Chauhan, P. Aggarwal, A. Karmarkar and K. K. Pandey, *Holz als Roh- und Werkst.*, 2001, **59**, 250–253.
- 29 Y. Iwamoto and T. Itoh, *J. Wood Sci.*, 2005, **51**, 595–600.
- 30 A. N. Papadopoulos, C. A. S. Hill and A. Gkaraveli, *Holz als Roh- und Werkst.*, 2004, **62**, 107–112.
- 31 R. M. Rowell and R. L. Youngs, *U.S. Department of Agriculture, Forest Service, Forest Products Laboratory*, 1981.
- 32 R. E. Ibach and R. M. Rowell, *Holzforschung*, 2001, **55**, 358–364.
- 33 W. L. E. Magalhaes and R. R. Da Silva, *J. Appl. Polym. Sci.*, 2004, **91**, 1763–1769.
- 34 Y. Zhang, S. Y. Zhang, D. Q. Yang and H. Wan, *J. Appl. Polym. Sci.*, 2006, **102**, 5085–5094.
- 35 C. Roussel, V. Marchetti, A. Lemor, E. Wozniak, B. Loubinoux and P. Gérardin, *Holzforschung*, 2001, **55**, 57–62.
- 36 Y. Li, *Advances in Composite Materials - Analysis of Natural and Man-Made Materials*, ed. P. Tesinova, InTech, Rijeka, 2011, ch. 9, pp. 229–284.
- 37 M. Schwarzkopf, *Wood Mater. Sci. Eng.*, 2021, **16**, 35–41.
- 38 M. Ghorbani, N. Poorzahed and S. M. Amininasab, *J. Compos. Mater.*, 2020, **54**, 1403–1412.
- 39 T. Meints, C. Hansmann and W. Gindl-Altmutter, *Polymers*, 2018, **10**, 81.
- 40 V. Siracusa, P. Rocculi, S. Romani and M. D. Rosa, *Trends Food Sci. Technol.*, 2008, **19**, 634–643.
- 41 A. K. Agrawal, *Spinning of Poly(Lactic Acid) Fibers*, 2010.
- 42 A. P. Gupta and V. Kumar, *Eur. Polym. J.*, 2007, **43**, 4053–4074.
- 43 K. Deng, H. Chen, Y. Zhao, Y. Zhou, Y. Wang and Y. Sun, *PLoS One*, 2018, **13**, e0201777.
- 44 P. I. Anakhu, C. C. Bolu, A. A. Abioye, G. Onyiagha, H. Boyo, K. Jolayemi and J. Azeta, *Arch. Foundry Eng.*, 2018, **18**, 65–71.
- 45 Z. Liu, Y. Wang, B. Wu, C. Cui, Y. Guo and C. Yan, *Int. J. Adv. Manuf. Technol.*, 2019, **102**, 2877–2889.
- 46 W. Shao, J. He, Q. Han, F. Sang, Q. Wang, L. Chen, S. Cui and B. Ding, *Mater. Sci. Eng., C*, 2016, **67**, 599–610.
- 47 T. Tsukegi, N. Naqasawa, T. Horii and H. Nishida, *Polym. Pap.*, 2015, **72**, 361–368.
- 48 A. Ashori, *Bioresour. Technol.*, 2008, **99**, 4661–4667.
- 49 H. P. Fink and J. Ganster, *Macromol. Symp.*, 2006, **244**, 107–118.
- 50 A. K. Mohanty, M. Misra and G. Hinrichsen, *Macromol. Mater. Eng.*, 2000, **276–277**, 1–24.
- 51 D. Plackett, T. L. Andersen, W. B. Pedersen and L. Nielsen, *Compos. Sci. Technol.*, 2003, **63**, 1287–1296.
- 52 M. Wollerdorfer and H. Bader, *Ind. Crops Prod.*, 1998, **8**, 105–112.
- 53 S. Wong, R. A. Shanks and A. Hodzic, *Macromol. Mater. Eng.*, 2004, **289**, 447–456.
- 54 A. Gondaliya, N. Alipoormazandarani, M. Kleiman and E. J. Foster, *Mater. Today Commun.*, 2023, **35**, 105846.
- 55 ASTM D4761 – 05, 2009, vol. i, pp. 1–11.
- 56 E. Aydin, J. A. Planell and V. Hasirci, *J. Mater. Sci.: Mater. Med.*, 2011, **22**, 2413–2427.
- 57 J. Ambrosio-Martín, M. J. Fabra, A. Lopez-Rubio and J. M. Lagaron, *J. Mater. Sci.*, 2014, **49**, 2975–2986.
- 58 D. Garlotta, *J. Polym. Environ.*, 2019, **9**, 63–84.
- 59 G. Kister, G. Cassanas and M. Vert, *Polymer*, 1998, **39**, 267–273.
- 60 H. Younes and D. Cohn, *Eur. Polym. J.*, 1988, **24**, 765–773.
- 61 M. Poletto, A. J. Zattera, M. M. C. Forte and R. M. C. Santana, *Bioresour. Technol.*, 2012, **109**, 148–153.
- 62 A. N. Shebani, A. J. van Reenen and M. Meincken, *Thermochim. Acta*, 2008, **471**, 43–50.
- 63 D. K. Shen, S. Gu and A. V. Bridgwater, *Carbohydr. Polym.*, 2010, **82**, 39–45.
- 64 A. Anca-Couce, N. Zobel, A. Berger and F. Behrendt, *Combust. Flame*, 2012, **159**, 1708–1719.
- 65 L. Burhenne, J. Messmer, T. Aicher and M. P. Laborie, *J. Anal. Appl. Pyrolysis*, 2013, **101**, 177–184.
- 66 H. Zhou, Y. Long, A. Meng, Q. Li and Y. Zhang, *Thermochim. Acta*, 2013, 36–43.



- 67 J. Y. Kim, S. Oh, H. Hwang, U. J. Kim and J. W. Choi, *Polym. Degrad. Stab.*, 2013, **98**, 1671–1678.
- 68 A. Khelifa, A. Bensakhria and J. V. Weber, *J. Anal. Appl. Pyrolysis*, 2013, **101**, 111–121.
- 69 M. Zhang, F. L. P. Resende, A. Moutsoglou and D. E. Raynie, *J. Anal. Appl. Pyrolysis*, 2012, **98**, 65–71.
- 70 M. Noël, W. J. Grigsby and T. Volkmer, *J. Wood Chem. Technol.*, 2015, **35**, 325–336.

